Comparison of cell wall chemical evolution during the development of fruits of two contrasting quality from two members of the Rosaceae family: Apple and sweet cherry

Marc Lahaye, Wafae Tabi, Lucie Le Bot, Mickaël Delaire, Mathilde Orsel-Baldwin, José Antonio Campoy, José Quero-Garcia, Sophie Le Gall

Comparison of cell wall chemical evolution during the development of fruits of two contrasting quality from two members of the Rosaceae family: apple and sweet cherry

Marc Lahaye*[a], Wafae Tabi[a,b], Lucie Le Bot[a,b], Mickael Delaire[c], Mathilde Orsel[c], José Antonio Campoy[d], José Quero Garcia[e], Sophie Le Gall[a,b]

[a] INRAE, UR BIA, 44300, Nantes, France

[b] INRAE, PROBE research infrastructure, BIBS Facility, F-44316 Nantes, France

c Univ Angers, Institut Agro, INRAE, IRHS, SFR QUASAV, F-49000 Angers, France

d Department of Plant Developmental Biology, Max Planck Institute for Plant Breeding Research, 50289 Cologne, Germany

e Univ. Bordeaux, INRAE, Biologie du Fruit et Pathologie, UMR 1332, F-33140 Villenave d'Ornon, France

∗Corresponding author. E-mail address: marc.lahaye@inrae.fr (M. Lahaye).

Abstract

Cell wall composition was studied during the development of apple cultivars (14-161/182 days after full bloom, DAA) maintaining firm fruit (Ariane) or evolving to mealy texture (Rome Beauty) when ripe and in sweet cherry cultivars (21/26-70/75 DAA) to assess their skin-cracking susceptibility (tolerant Regina and susceptible Garnet).

Pectin sugar composition and hemicellulose fine structure assessed by enzymatic degradation coupled to MALDI-TOF MS analysis were shown to vary markedly between apples and cherries during fruit development. Apple showed decreasing rhamnogalacturonan I (RGI) and increasing homogalacturonan (HG) pectic domain proportions from young to mature fruit. Hemicellulose-cellulose (HC) sugars peaked at the beginning of fruit expansion corresponding to the maximum cell wall content of glucose and mannose. In contrast, HG peaked very early in the cell wall of young developing cherries and remained constant until ripening whereas RGI content continuously increased. HC content decreased very early and

remained low in cell walls. Only the low content of mannose and to a lesser extent fucose increased and then slowly decreased from the beginning of the fruit expansion phase. Hemicellulose structural profiling showed strong varietal differences between cherry cultivars. Both apples and cherries demonstrated a peak of glucomannan oligomers produced by β-glucanase hydrolysis of the cell wall at the onset of cell expansion. The different glucomannan contents and related oligomers released from cell walls are discussed with regard to the contribution of glucomannan to cell wall mechanical properties. These hemicellulose features may prove to be early markers of apple mealiness and cherry skin-cracking susceptibility.

Keywords: *Malus domestica*, *Prunus avium*, pectin, hemicellulose, fruit-cracking, fruit texture

1 Introduction

The Rosaceae family encompasses many economically important fruits, such as apple, cherry, peach, and strawberry, which need to meet several qualitative criteria for consumers and processors. Among them mechanical properties are particularly important with regard to texture and fruit resistance to external stresses. During fruit development, various biotic and abiotic stresses can alter the setup of tissues with consequences for their quality once ripe. The role of these stresses in terms of the variability of quality in cultivars between harvest years is an important question considering climate fluctuations. This variability makes the identification of stable genetic markers useful in breeding programs to improve quality and, notably, texture particularly difficult [1]. Full understanding and control of these variations remain a challenge to date. One issue is understanding the cell wall construction and evolution during fruit development, as these are central in determining tissue mechanical properties involved in fruit quality. Cell walls, composed of an assembly of pectin, hemicellulose and cellulose polysaccharides, provide cell-cell adhesion and mechanical resistance to withstand cell turgor pressure [2]. During apple fruit development from young to mature fruit, firmness declines [3] with the remodeling of cell wall polysaccharides, ending with their disassembly by complex enzyme consortia and nonenzymatic mechanisms [4, 5]. Pectin is a major determinant of fruit mechanical properties [6, 7]. As an example, infusion of various specific enzymes targeted toward cell wall polysaccharides degradation showed that cellulose and hemicellulose were involved in the viscoelastic mechanical properties of apple flesh but to a lesser extent than pectin [8]. Moreover, several fruit enzymes degrading pectin are directly related to fruit softening [6, 9-12]. The contribution of pectin structural domains bearing galactan and arabinan side chains (rhamnogalacturonan I, RGI) to fruit texture is also well documented [6]. In fact, homogalacturonan (HG) and side chains of RGI pectin structural domains interact with cellulose and are thought to contribute to cell wall mechanical properties [13]. RGI side chains appear to be beneficial to the firmness of turgid apple fruit but not for plasmolyzed tissue [14]. These side chains were proposed to make analogous contributions to the cell wall mechanical properties, as the minor fraction of xyloglucan hemicellulose (XyG) which interacts with cellulose and forms biomechanical hotspots [15]. The side chains would control the sliding of cellulose microfibrils in the cell wall under the tension stress of turgid cells. HG hydration and cellulose organization are related to cell wall poroviscoelastic mechanical properties [14], for which the water flux controlled by pectin in the porous cell wall contributes to the wall mechanical properties [7].

In apple, more pectin is hydrated, more cellulose microfibrils are dispersed, and the storage modulus is higher. In light of these data, the role of bulk hemicellulose in cell wall mechanical properties remains unclear. It is expected that hemicellulose will compete with pectin [16] and interact with other cell wall polymers depending on their fine structure, such as acetyl esterification, which is known to affect hydrogen binding of glucuronoxylan (GuX) or galactoglucomannan (GgM) hemicelluloses to cellulose [17]. The molecular weight of XyG has also been shown to affect cellulose binding and swelling of XyG-cellulose model assembly [18]. As hemicellulose is under continuous remodeling during fruit development [19, 20], it is thought that these genetically and environmentally controlled changes are required during the setup and reorganization of cellulose and pectin in cell wall of the developing fruit. In the present study, the kinetics of cell wall composition and hemicellulose structural changes from young to ripe apple (*Malus domestica*) and sweet cherry (*Prunus avium*), two members of Rosaceae, were followed. Hemicellulose structural profiling was realized by coupling the degradation of cell wall polysaccharides by an endo-β-D-glucanase with MALDI-TOF MS analysis of the hydrolysate, an approach that has been previously shown to be sensitive to reveal plant cell wall polysaccharide structural variations according to organ development and plant genetics [19, 21, 22]. Cultivars of apple developing contrasting firmness when ripe were chosen, namely, Ariane (firm) and Rome Beauty (soft to mealy when overripe) [23]. Sweet cherry cultivars differing in their susceptibility to skin cracking were selected, namely, Regina (tolerant) and Garnet (susceptible) [24]. Apple and cherries were also selected for their remarkably different brittle versus soft and melting textures, which are usually related to differential cell wall swelling and pectin metabolism [25]. This analysis allowed testing to determine whether the cell wall setup during early fruit development differed in the texture and skin-cracking of ripe fruits.

2 Materials and methods

2.1 *Fruit*

2.1.1 Apple

Apple fruits were harvested in 2014 from six-year-old apple trees of Ariane and Rome Beauty cultivars trained under normal production conditions in an experimental orchard at the INRAE experimental unit in Beaucouzé, France (47°28'N, 0°33'W). For both cultivars, fruits were harvested at 14, 28, 42, 56, 84, and 98 days after blooming and at commercial harvest

(161 and 182 days after blooming for Ariane and Rome Beauty, respectively). At harvest, mature fruit were also kept at 2 °C for 2 months.

For each date, fruits were separated into 6 or 12 batches composed of 2 to 5 fruits collected from different trees. For the first harvest date and due to the small size of the fruits, only one batch composed of 9 fruits was formed. For each batch, fruits were cut up to form one sample composed of fruit pieces, immediately frozen in liquid nitrogen and stored at −80 °C before use.

Fruit harvest dates were expressed as cumulative growing degree-days (DD) from the date of full bloom to consider the differences between both cultivars in terms of dates of anthesis. For each day, DD was calculated as the difference between the daily mean temperature and a base temperature of 7 °C, as proposed previously [26]. The cumulative DD obtained for a harvest date was then calculated as the sum of DD from the day of full bloom to this harvest day using daily air temperatures (°C) obtained from a local weather station. For cold stored fruits, DD was calculated by adding 120 units (i.e., 60 days at 2 °C) to the DD calculated at commercial harvest.

2.1.2 Cherries

Garnet and Regina cherry cultivars were harvested in 2015 at eight different dates corresponding to 26, 32, 40, 49, 56, 62, 69 and 75 days after blooming for Garnet and 21, 27, 35, 44, 51, 57, 64 and 70 days after blooming for Regina. Trees were cultivated at the Tree Experimental Unit (UEA) of the INRAE-Bordeaux research center in Toulenne, 50 kms southeast from Bordeaux, France (44°57' N, 0°28 W'). The plot where trees were studied was highly homogeneous in terms of soil composition and horticultural practices. For each cultivar, four trees were sampled, two of which were planted together in two different plots. Trees from Regina were 3 and 8 years old and from Garnet were 3 and 9 years old. For each date, fruits from each cultivar and plot were pooled. At harvest, fruits were placed in cryogenic tubes of 40 mL, immediately frozen in liquid nitrogen, and then stored at -80 ℃. Pits were removed using mortar and pestle. After pit removal, each sample was ground using an automatic mortar grinder with a high thermic inertia. Ground material was aliquoted with 5 g for each sample used for sample analyses. Overall, three technical replicates were made for each biological replicate (or each considered plot). For each cultivar and sample date, between 10 and 20 fruits were individually weighed.

For apple, harvest dates were expressed as DD from the date of full bloom. The same base temperature of 7 °C was considered.

147

148 2.2 *Cell wall preparation*

149 Apple outer cortex and cherry exocarp pieces (free of pit and stone) were freeze-dried and
150 dried at 40 °C for 2 h under vacuum over P_2O_5 before weighing and powdering (FastPrep24,
151 MP Biomedicals; 6.5 $m.s^{-1}$ for 60 s). Cell walls were prepared as alcohol insoluble material
152 (AIM) from powder using an Automatic Solvent Extractor (ASE® 350, Thermo Scientific) as
153 reported previously [23]. AIMs were dried at 40 °C overnight under vacuum over P_2O_5 before
154 weighing in order to determine the extraction yield. AIMs were ground before chemical
155 analyses.

156

157 2.3 *Polysaccharide composition*

158 Sugar composition in AIM was assessed after two steps of hydrolysis in sulfuric acid (72% at
159 RT for 30 min followed by 2 M at 100 °C for 120 min) [23]. Neutral sugars were analyzed by
160 GC using a Trace GOLD TG-225 GC Column (30 x 0.32 mm ID) on a TRACE^{TM} Ultra Gas
161 Chromatograph (Thermo Scientific; temperature 205 °C, carrier gas H_2) after conversion to
162 alditol acetates, as reported previously [23]. Sugar standard solution and inositol were used
163 for calibration and as internal standards, respectively. Uronic acids in acid hydrolysates were
164 analyzed by colorimetry with meta-hydroxydiphenyl, as reported previously [23].
165 Starch measurement in AIM was performed after amylolysis and HPAEC analyses as
166 described in [27].

167

168 2.4 *Hemicellulose enzymatic profiling*

169 Cell wall material was degraded by commercial endo-1,4-β-glucanase from *Trichoderma*
170 *longibrachiatum* (Megazyme, Bray, Ireland; 20 U) overnight at 40 °C under agitation, as
171 reported previously [23]. Oligosaccharides in the hydrolysates were analyzed by MALDI-
172 TOF MS in positive mode using an Autoflex III MALDI-TOF/TOF spectrometer (Bruker
173 Daltonics, Bremen, Germany), as reported previously [23]. One or three replicates per
174 hydrolysis were mixed with the ionic liquid matrix DMA/DHB and deposited on MTP 384
175 polished steel. The instrument was externally calibrated using galactomannan oligomers (DP
176 3–9) of known mass. Spectra were recorded in the mass range m/z 500–2000. Spectra were
177 exported to Flex Analysis 3.4 software (Bruker) and preprocessed. Mass lists reporting m/z
178 (monoisotopic masses, after deisotoping with the SNAP algorithm, Bruker) and intensities of
179 detected ions were then exported to R software [28] for statistical analysis and graphical
180 representation. Ion masses and intensities of the spectra of glucanase hydrolysates were

normalized to that of the XXXG ion at m/z 1085. Identification of ions was performed by comparison with the m/z list of theoretical masses of the sodium adduct of different oligosaccharides. Ion attribution to xyloglucan structures was performed on the basis of combinations of hexose, methyl-pentose, pentose, hexuronic acid and acetyl ester substituents. The nomenclature of oligomers of xyloglucan released by glucanase followed that of [29] and is summarized in **Fig S1**. Briefly, bare (1,4)-linked β-D- glucose residues were noted as G. Extension of glucose by (1,6)-linked α-D-xylose was noted as X. Further extensions on the xylose residues on O-2 by β-D-galactose or α-D-fucosyl-(1->2)-β-D-galactose were noted as L and F, respectively. When a hexuronic acid residue is present, it is indicated by the letter Y, while the presence of two contiguous xylosyl groups on the glucose backbone is noted as U. For other oligomers, Hex and Pen refer to hexose and pentose, respectively, followed by the number of these residues in the oligomer (see **Table S1**). Acetyl-esterification of structures was noted as "a" while the presence of hexuronic acid and a methyl ether was noted by "u" and "m" respectively. The number following the code corresponds to the number of sugar or substituent groups. For example, Pen2u1m1a1 corresponds to a dimer of pentose with one hexuronic acid, one methyl ether and one acetyl group.

2.5. *Data analysis*

All statistical analyses were performed using R [28]. These included standard error of the mean and principal component analysis (PCA) calculation of data replicates. The number of replicates is indicated in figure and table legends. Due to the different degree-days of the samples, significant differences in data between varieties were based on the comparison of the 95% confidence interval estimated from the standard error of the mean x 1.96. Ellipses on individual PCA plots corresponded to the 95% confidence location of the data barycenter according to [30].

MS data were analyzed by an in-house script in R used previously [19, 20, 22, 31, 32]. This script tabulated m/z values and peak intensity from spectra exported as text files from the mass spectrometer. The same script associated the m/z value with a known or calculated mass values for oligosaccharides (**Table S1**) prior to statistical analyses.

All MS spectra were normalized to the intensity of the XyG ion XXXG (1085 m/z) to correct for differences in intensities between spectra. PCA of MS data from glucanase hydrolysate were also scaled to zero mean and unit variance.

3 Results

3.1 *Cell wall compositions of firm and soft apple cultivars differ and are markedly affected by development*

Rome Beauty fruits developed into larger fruits than Ariane fruits (**Fig S2A**). The fruit dry weight content first decreased in young fruits of both cultivars until approximately 250 degree-days (DD) and then increased steeply up to approximately 750 DD to increase more slowly later on (**Fig S2B**). After approximately 500 DD, by comparing estimated confidence intervals from the standard error of the means, Ariane was significantly richer in dry matter than Rome Beauty, likely due in part to the lower amount of water compared to the large Rome Beauty fruits. Ariane fruits were also enriched in dry matter during postharvest storage. The alcohol insoluble material representing polymeric material decreased in young fruits along with dry material before a rebound at approximately 250 DD to reach a maximum at approximately 750-1000 DD before a marked decrease during fruit expansion (**Fig S2C**). Nonpolysaccharide polymeric material (most likely mainly protein; AIM subtracted from nonstarch polysaccharides and starch; **Fig S2D**) was at its highest level in the very young fruits (approximately 60% AIM dw) and decreased to approximately 10% after approximately 700 DD. Starch started to accumulate from approximately 250 DD to a maximum at approximately 750-1000 DD before markedly decreasing thereafter and notably during storage (**Fig S2E**). Nonstarch polysaccharides corresponding to cell wall material followed the opposite behavior with an enrichment during storage. Between 500 and 1000 DD starch and cell wall contents in Ariane were significantly higher and lower than Rome Beauty, respectively (**Fig S2F**).

The mean sugar composition of nonstarch polysaccharides (NSP) considering all the developmental stages and both cultivars was glucose (**Table S2;** 33.9% of AIM dry weight), uronic acid (25.3%), arabinose (14.6%), galactose (14.0%), xylose (5.0%), mannose (3.4%), rhamnose (1.3%) and fucose (0.8%). This composition changed during fruit development, as particularly shown by principal component analysis capturing 77.5% of the variance in the first two components (PCA; **Fig 1A**). Young developing fruit were characterized by an increase in galactose and mannose content up to approximately 500 DD and a concomitant decrease in arabinose, rhamnose, uronic acid and xylose contents (**Fig. 1B**). The glucose content increased up to 850 DD for Ariane and 960 DD for Rome Beauty before decreasing along with mannose and galactose contents to benefit an increase in uronic acids, xylose and

fucose. The proportion of the three latter sugars distinguished the late development phases (**Fig 1, Table S2**). Of interest are the negative correlations between the glucose content and those of rhamnose and arabinose, the absence of a relation between galactose and mannose with rhamnose and glucose (orthogonal positions) and the collinearity of mannose and galactose contents (**Fig 1A**). There appears to be antagonism between pectic RGI structural domains rich in rhamnose and either RGI arabinose side chains and/or arabinogalactan proteins with cellulose, xyloglucan (XyG) and/or galactoglucomannan (GgM) contents. These results also indicated a disjunction of galactose metabolism distinguishing RGI galactan side chains from RGI arabinan side chains. An antagonism between the metabolism of GgM and XyG hemicelluloses, taking fucose and xylose as markers of XyG appeared with development. Rome Beauty tended to be richer in glucose and mannose and poorer in uronic acids, rhamnose, fucose and xylose.

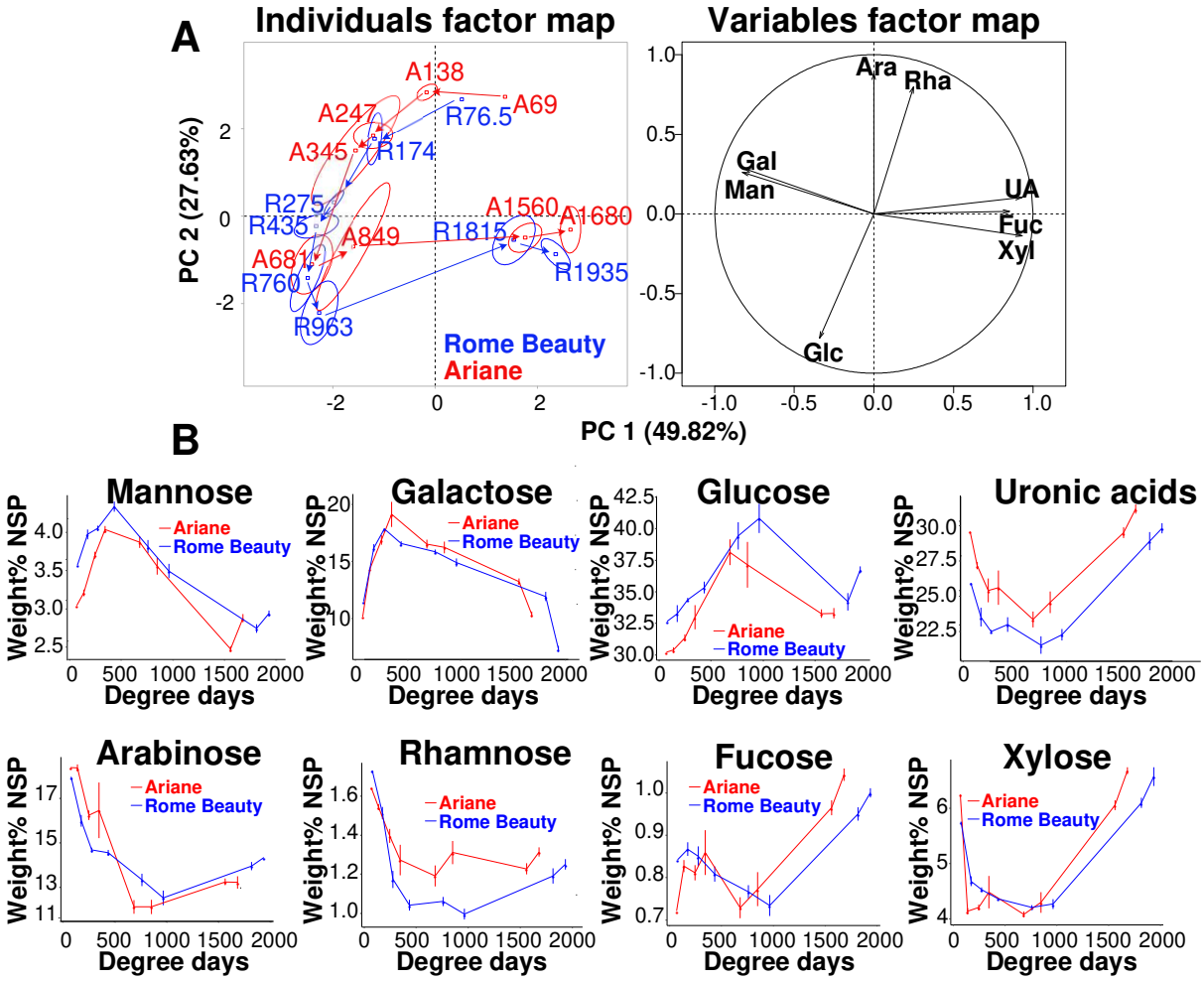

Figure 1 Principal component analysis (A) and variations in sugars content in nonstarch polysaccharides (B) according to Ariane and Rome Beauty apple development. Ellipses in (A) are 95% confidence ellipses for the barycenter of individuals; arrows in (A) and lines in (B)

are aids for the eyes to follow changes with fruit development; bars: standard error; n = 1 (pool of 9 fruits), 6, 6, 6, 6, 6, 12, 12 fruits for both Ariane and Rome Beauty.

Considering molar proportions of cell wall sugars, the major turning points noticed on the PCA map of individuals at approximately 850 and 960 DD for Ariane and Rome Beauty, respectively, corresponded to the maximum molar proportion of cellulose and hemicellulose sugars (HC) and to the lowest proportion of HG pectic domains (**Fig 2A, 2B**). In agreement with the sugar composition of the NSP, Rome Beauty was richer in HC and poorer in pectic HG domains than to Ariane. The molar proportion of the RGI pectic domain was close in the two cultivars and decreased after a maximum at approximately 250-500 DD (**Fig 2C**). However, considering the HG and RGI pectic domains together, the Rome Beauty cell wall pectin was richer in RGI, and Ariane showed a higher proportion of HG domains (**Fig 2D**). Nevertheless, the ratio of pectin to hemicellulose and cellulose was close for the two cultivars: the richness in HG pectic domains in Ariane compensated for its sparseness in HC (**Fig 2E**). Assuming that arabinose and galactose were all part of pectic RGI neutral side chains linked to rhamnose, the richness in rhamnose for Ariane (**Fig 1B**) led to shorter side chains according to their molar ratio (**Fig 2F and G**). However, considering only these side chains, their ratio indicated that Ariane was richer in galactan side chains from approximately 500 DD until harvest (**Fig. 2H)**.

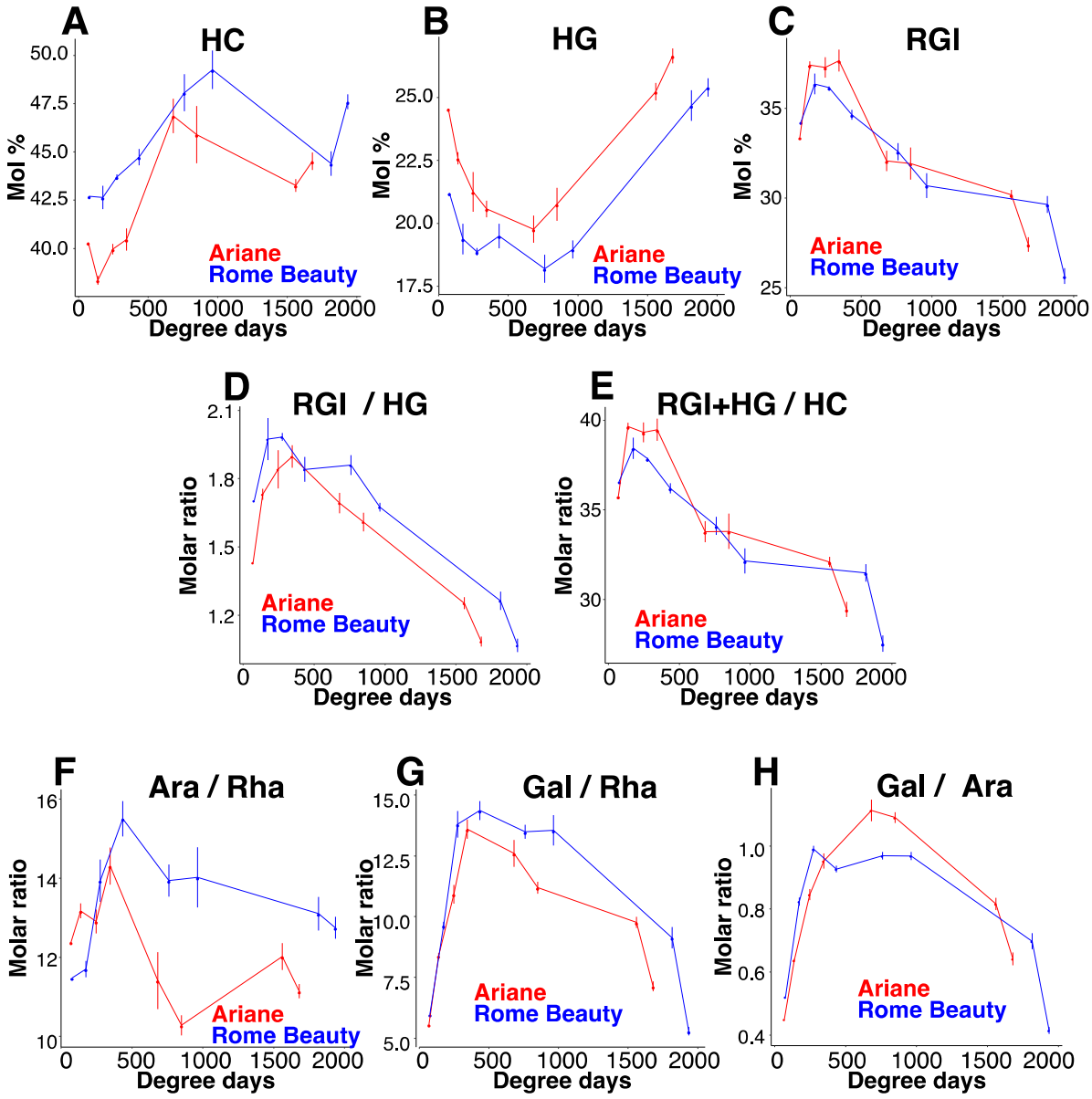

Figure 2 Cell wall sugar molar percentage ratio: (A) hemicellulose and cellulose (HC; Glc+Xyl+Man+Fuc mol%), (B) homogalacturonan (HG; uronic acids – Rha mol%), (C) rhamnogalacturonan I (RGI; Ara+Gal+Rha mol%), (D) ratio of RGI/HG pectic domains, (E) ratio of pectin to cellulose and hemicellulose, (F) arabinose to rhamnose mol%, (G) galactose to rhamnose mol%, and (H) ratio of RGI side chains in Ariane and Rome Beauty according to development. Lines are aids for the eyes bars: standard errors; n = 1 (pool of 9 fruits), 6, 6, 6, 6, 6, 12, 12 fruits for both Ariane and Rome Beauty.

The hemicellulose structural profile resulting from glucanase degradation coupled to MALDI-TOF mass spectrometry consisted of XyG oligomers and acetylated hexose oligomers attributed in part to GgM and glucan (**Fig 3**). The variation in their relative proportion

297 confirmed their structural evolution with apple development. GgM/glucan oligosaccharides
298 contributed more than XyG to distinguish profiles by PCA in the early developmental stages
299 **(Fig 4)**. The PCA of the normalized ion intensity of oligosaccharides relative to that of the ion
300 of the XXXG structure released by glucanase accounted for 61.2% of the variance in the first
301 two components. It clearly showed a turning point at approximately 680 DD for Ariane and
302 between 435-760 DD for Rome Beauty on the individual map and was mainly attributable to
303 the variation in the contribution of GgM/glucan oligomers to the MS profiles. Changes were
304 also noticed at the same developmental stage for XyG structures, such as for XLFGa1, which
305 reached its maximum contribution, while XLFG reached its minimal contribution and
306 plateaued at low relative proportions thereafter (**Fig 4A, 4B; Table S3**). The two cultivars
307 differed: GgM/glucan oligomers contributed more to the Rome Beauty glucanase
308 oligosaccharide profile than Ariane oligomers, while XLXGa1 and XLFGa1 structures
309 distinguished the Ariane and Rome Beauty profiles, respectively (**Fig 4B; Table S3**). The
310 third and fourth components accounting for 14.3% of the variance did not distinguish
311 varieties or development (sup Fig).
312

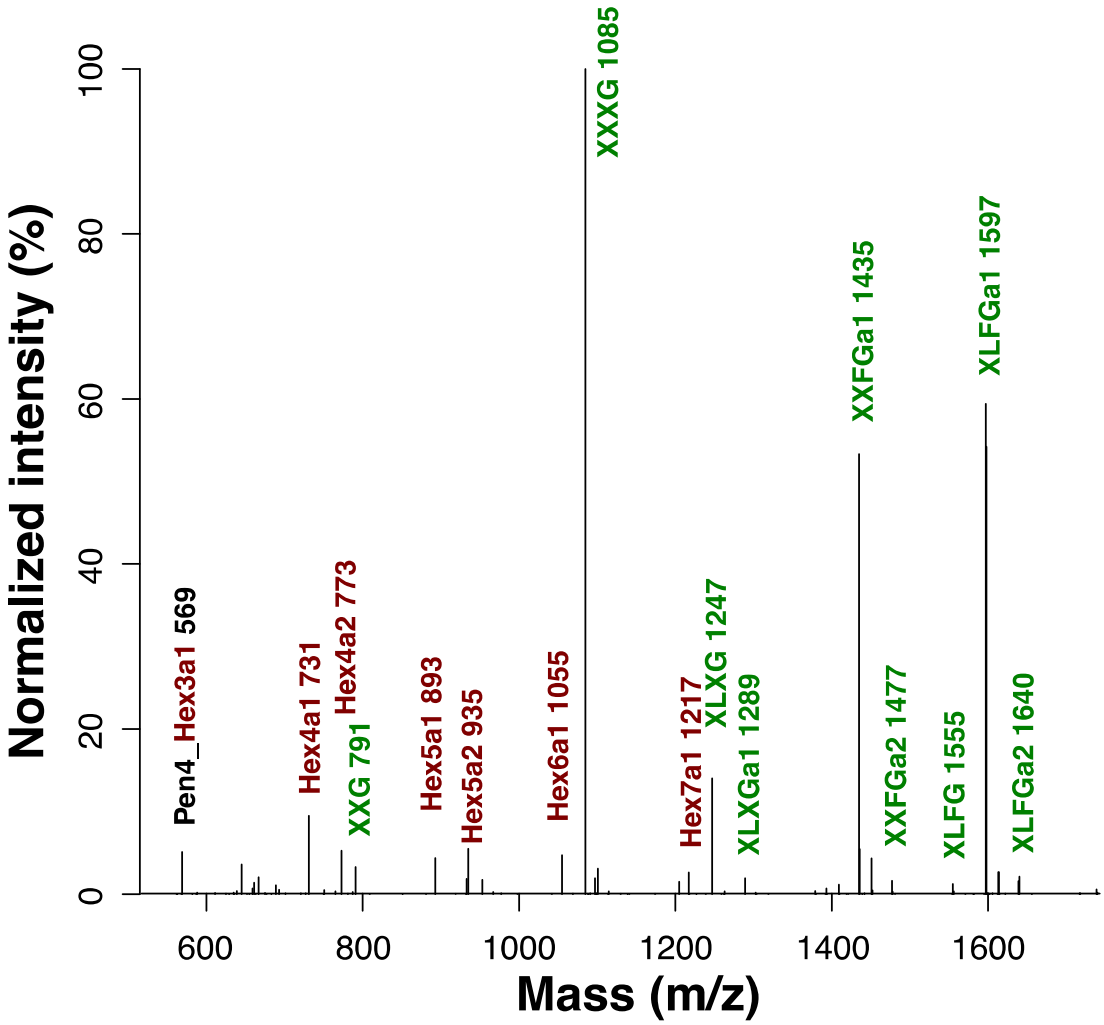

Figure 3 Average MALDI-TOF MS spectrum of apple glucanase hydrolysate from the entire fruit collection (n = 330). The nomenclature is as described in the text, in Table S1 and Figure S1 followed by the m/z value; in brown: hexose-based oligomers attributed to GgM/β-glucan, in green: XyG oligomer; black: pentose-based oligomers attributed to glucuronoarabinoxylan/glucuronoxylan (GAX/GuX). The intensity of ions was normalized to that at m/z 1085 attributed to the XyG structure XXXG.

Thus, the cell wall composition and the hemicellulose structure differed between the soft and firm cultivars. Rome Beauty had higher proportions of cellulose/hemicellulose, whereas Ariane was richer in HG pectic domains. Further differences were noted in the pectic RGI domains with longer side chains for Rome Beauty but more frequent galactan side chains for Ariane. Aside from these varietal differences, the kinetics of cell wall construction and modification showed differences between the two cultivars. They both showed “turning

329 points" with regard to compositional changes in hemicellulose, cellulose and pectin and
330 hemicellulose structure with fruit development. Up to approximately 500 DD, RGI pectic
331 domains were the highest, while HG domains reached a minimum that remained until 1000
332 DD, at which point they increased to reach their maximum at harvest/postharvest for both
333 cultivars. The main difference with regard to sugars attributed to pectin concerned the molar
334 ratio of arabinose to rhamnose, which increased for the two cultivars up to 400-500 DD but
335 then markedly decreased for Ariane to reach its lowest value at approximately 1000 DD to
336 increase to a second maximum at approximately 1500 DD, while for Rome Beauty, the
337 decrease was less steep and more continuous. Kinetics of hemicellulose and cellulose changes
338 in proportion also distinguished Ariane and Rome Beauty. These polysaccharides increased
339 from approximately 250 DD to reach a maximum at 600 DD for Ariane and 1000 DD for
340 Rome Beauty to decrease thereafter until harvest before another enrichment during storage.
341 With regard to hemicellulose fragments following glucanase hydrolysis of cell walls, no
342 marked difference was observed in the kinetics of changes between Ariane and Rome Beauty.
343 The main "turning point" after approximately 345-850 DD corresponded to the maximum of
344 hemicellulose/cellulose.
345

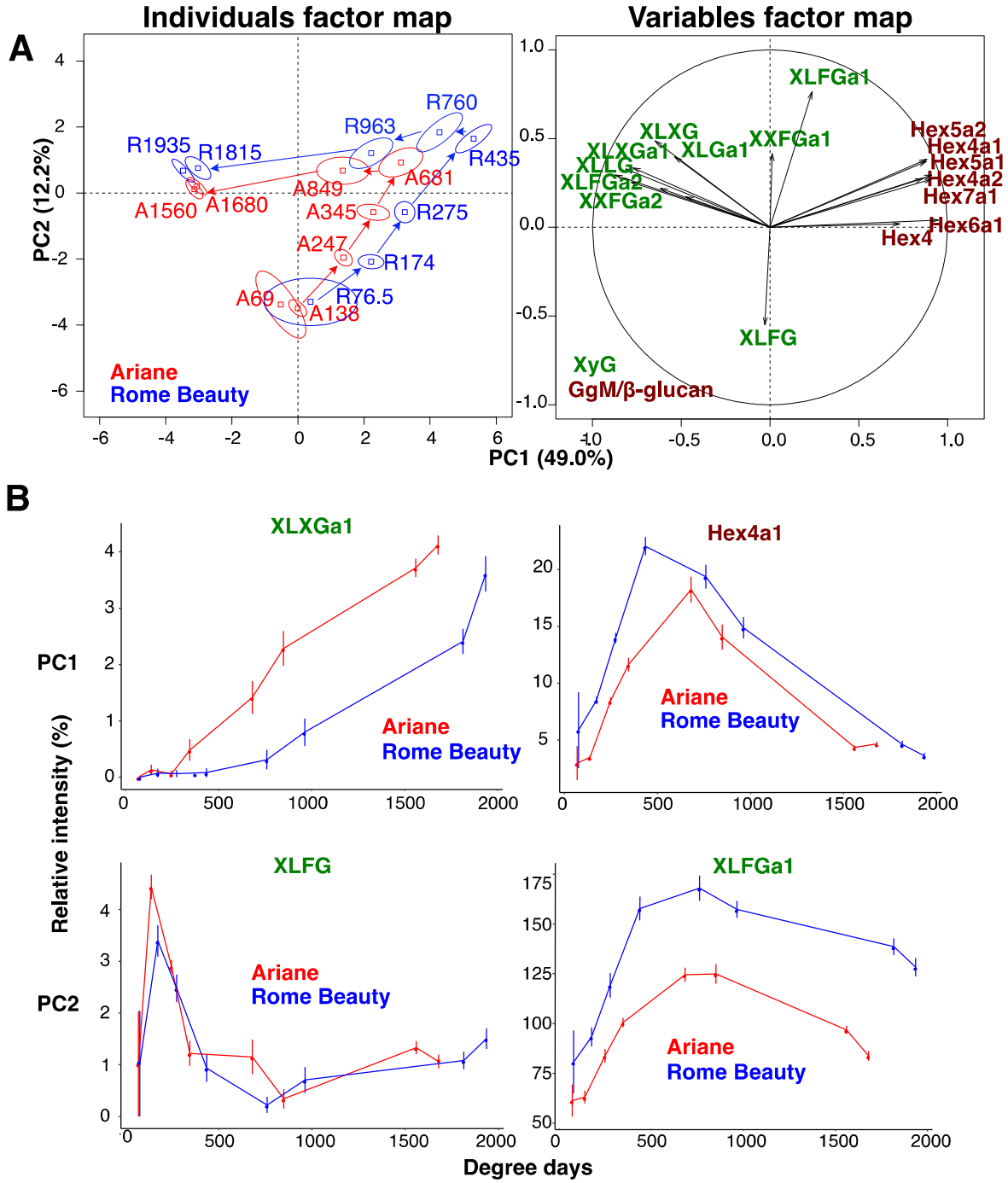

Figure 4 Principal component analysis of MALDI-TOF MS ions attributed to hemicellulose oligomers in the glucanase hydrolysate of AIM from Rome Beauty (R) and Ariane (A) according to development (the number following the letter corresponds to the degree-days). A) Principal components 1 and 2 (PC1, PC2), maps of individuals and variables; B) Variation in relative intensity of characteristic oligosaccharides contributing to PC1 and PC2. Nomenclature is as described in the text, Table S1 and Fig S1; ellipses in (A) are 95% confidence ellipses for the barycenter of individuals ; arrows in (A) and lines in (B) are

indicated to guide the eyes to follow changes with fruit development; bars: standard errors; n = 1, 6, 6, 6, 6, 6, 12, 12 fruits x instrumental triplicates for a total of 3, 18 or 36 repetitions for both Ariane and Rome Beauty.

3.2 *Sweet cherry cell walls are rich in pectin, and proportions in HG and RGI structural domains are markedly affected by fruit development*

Cherry fruits, characterized by double sigmoid growth, (**Fig S3A**), yielded alcohol insoluble material (AIM) from 6 to 50% of the initial dry powder (**Fig S3B**). Recovery significantly decreased according to cultivar at the different dates of collection. The increase in the overall fresh weight and the decrease in AIM during fruit growth were similar to those reported [33]. From approximately 300 DD to 550 DD, the cultivar Regina yielded significantly more AIM than Garnet ($p<0.01$). The overall sugar content varied significantly from 56 to 74% of the AIM dry weight according to the collection period but irrespective of the cultivar (**Fig S3C**). The lowest cell wall sugar content was observed in fruit collected at 512 DD for Garnet and at 472 DD and 554 DD for Regina.

The average cherry AIM was composed of uronic acids (27%), glucose (16%), arabinose (10%), xylose (5%), galactose (4%), mannose (2%) rhamnose (1%) and fucose (0.3% on the dry weight basis of AIM; **Table S4**). Principal component analysis of sugar composition captured 86.6% of the variance in the first two components. There were marked changes during fruit development, with a turning point at approximately 250-450 DD (**Fig 5A**). These changes were primarily due to a marked increase in the content of mannose and uronic acids up to date 3 and a marked decrease in glucose and xylose contents up to approximately 300-350 DD (**Fig 5B**). In addition, the contents of arabinose and galactose continuously increased throughout the collection period but showed a transient maximum at 300-350 DD followed by a decrease up to 450-550 DD before increasing until the end of the collection. There was no major difference in sugar content between the two cultivars during development except mannose content, which was higher in Regina compared to Garnet, and, to a lower extent, that of fucose and rhamnose between 300-500 DD.

Considering the molar percentage of sugar representative of the hemicellulose/cellulose (HC) and RGI and HG pectic domains, HC was a major contributor to sweet cherry cell walls in young fruit (**Fig 6A**) but rapidly decreased to low values after 300-350 DD to the benefit of the RGI and HG pectic domains (**Fig 6B, 6C**). The HG proportion increased and plateaued after 300-350 DD, while the RGI proportion still progressed until the

end of the collection. There were no major differences in the pectic domains between the two cultivars, and the RGI/HG ratio increased steadily throughout fruit development (**Fig 6D**). Likewise, the molar ratio of sugar attributed to pectin relative to cellulose and hemicellulose steadily increased to level off after approximately 600 DD (**Fig 6E**). With regard to the RGI, assuming that all galactose and arabinose were part of the side chains linked to rhamnose, the proportion of arabinose and galactose to rhamnose progressed until 300-350 DD and then plateaued. There was no major difference in the evolution of these ratios between Regina and Garnet during fruit development (**Fig 6F, 6G**). Considering similar rhamnose contents in the early development of the two cultivars (approximately 300 DD, **Fig 5**), Regina presented longer Gal side chains (**Fig 6H**). Such differences disappeared in later developmental stages. Thus, similar to apple, sweet cherry cell wall composition markedly changed during fruit development. However, unlike apple, the two sweet cherry cultivars did not differ in the kinetics of cell wall composition changes during development. They markedly differed from apple with a much lower contribution of cellulose/hemicellulose to the cell wall (approximately 6 mol% for sweet cherries for approximately 52 mol% in ripe apples), although they shared close global pectin structural domain composition with approximately 50 mol% HG for ripe sweet cherries and 48 mol% in ripe apples.

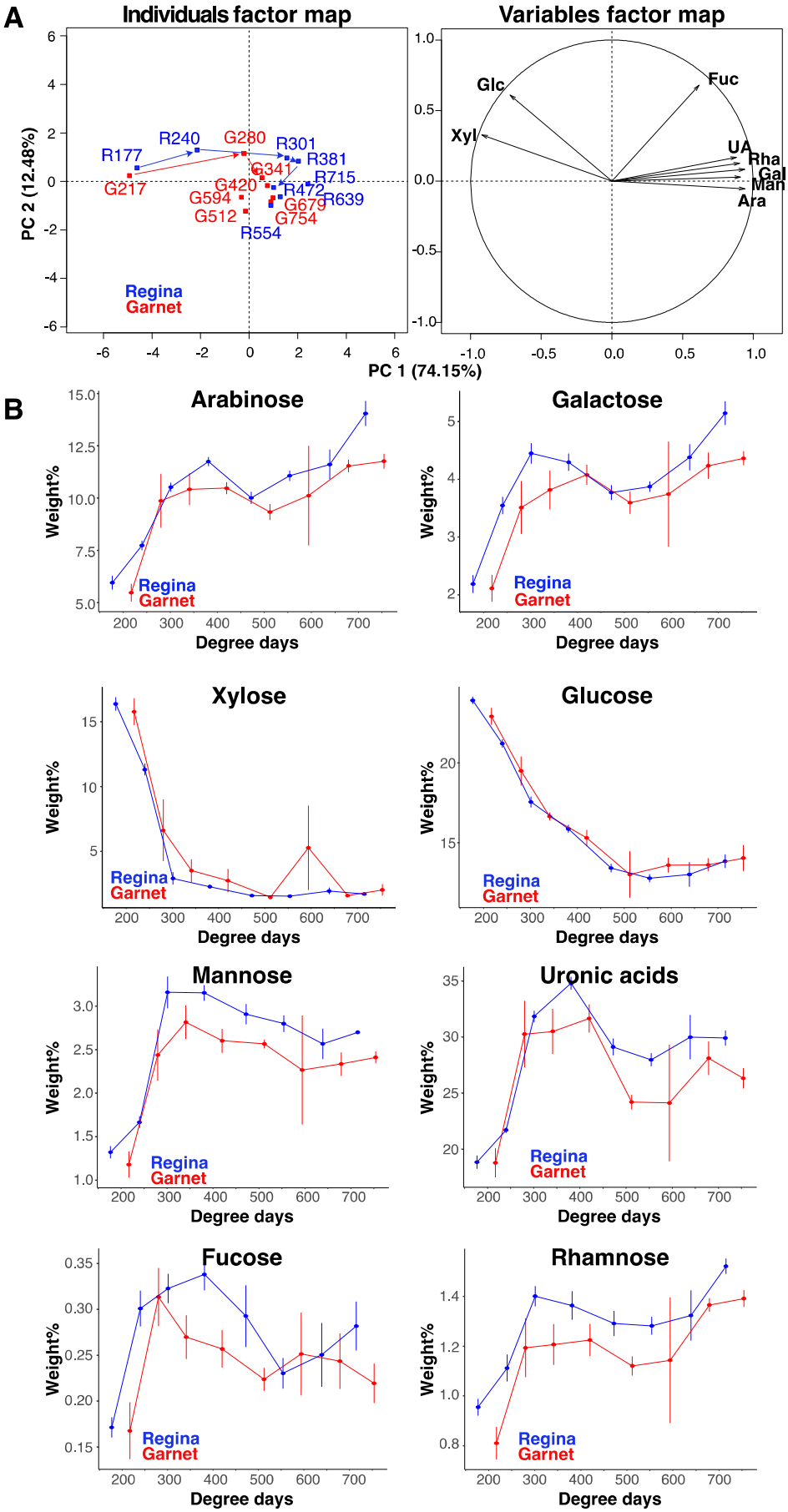
A
Individuals factor map
Variables factor map
PC 2 (12.48%)
PC 1 (74.15%)
R177
R240
G280
R301
R381
G341
R715
G217
G420
R472
G594
G679
R639
G512
G754
R554
Regina
Garnet
Glc
Fuc
Xyl
UA
Rha
Gal
Man
Ara
B
Arabinose
Galactose
Xylose
Glucose
Mannose
Uronic acids
Fucose
Rhamnose
Weight%
Degree days
Regina
Garnet

407

Figure 5 Principal component analysis (A) and variations in sugars content in nonstarch polysaccharides (B) according to Regina and Garnet sweet cherry development. Arrows in (A) and lines in (B) are aids for the eyes; bars: standard error; n = 6 except G4 n =3 and G6 n = 5.

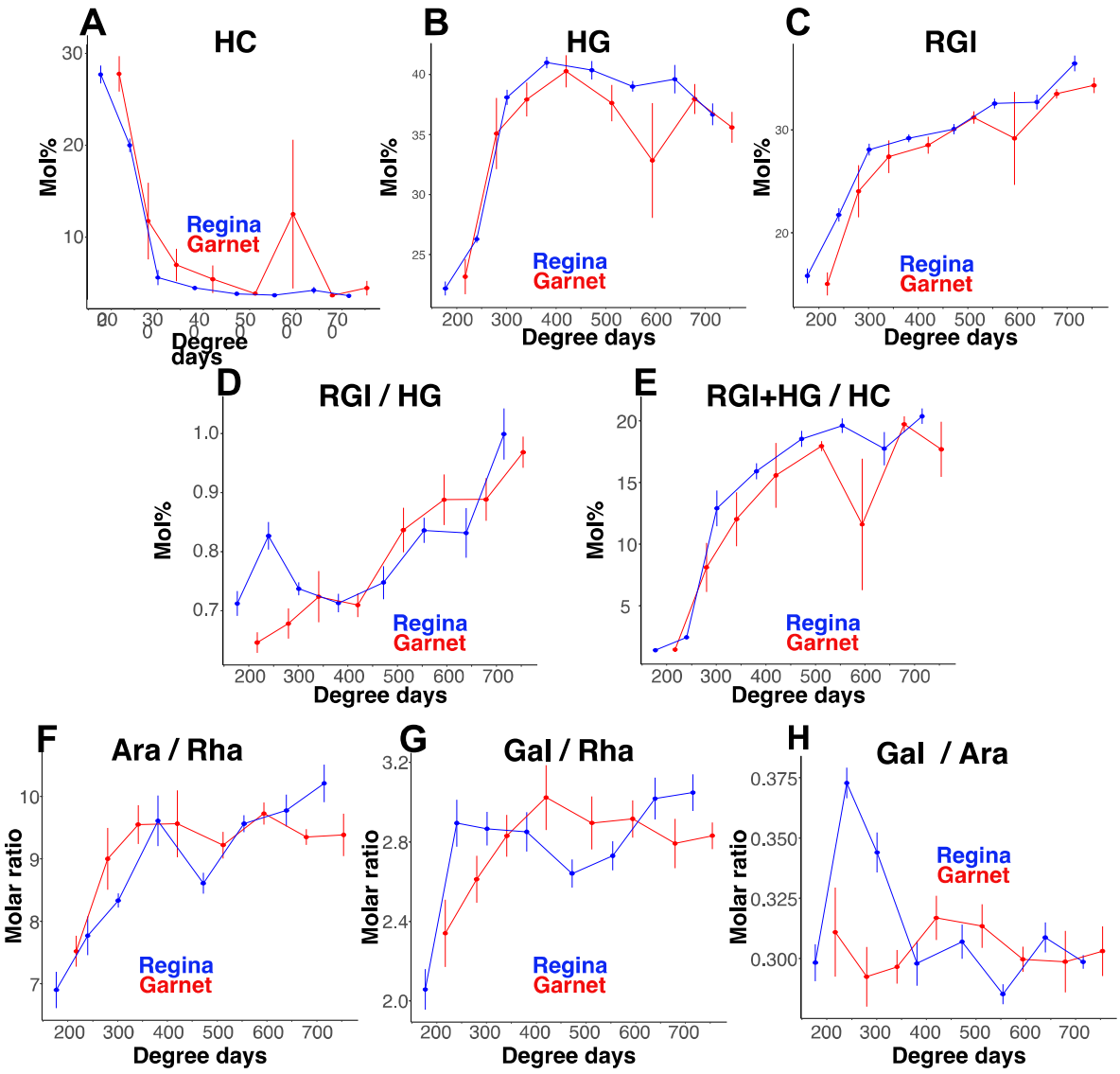

Figure 6 Cell wall sugar molar percentage ratio: (A) hemicellulose and cellulose (HC; Glc+Xyl+Man+Fuc mol%), (B) homogalacturonan (HG; uronic acids – Rha mol%), (C) rhamnogalacturonan I (RGI; Ara+Gal+Rha mol%), (D) ratio of RGI/HG pectic domains, (E) ratio of pectin to cellulose and hemicellulose, (F) arabinose to rhamnose mol%, (G) galactose to rhamnose mol%, and (H) ratio of RGI side chains in Regina and Garnet according to development. Lines are aids for the eyes, bars: standard error; n = 6 except G4 n =3 and G6 n = 5.

Hemicellulose degradation by endoglucanase released oligomers that were attributed by MALDI-TOF MS on the basis of m/z. A typical MS spectrum is shown in **Fig. 7**. It differed from apple by the presence of unusual oligomers containing uronic acid (XXYG and potentially XULG, which is isobar with Hex8a1) and an unknown oligosaccharide at m/z 1107.

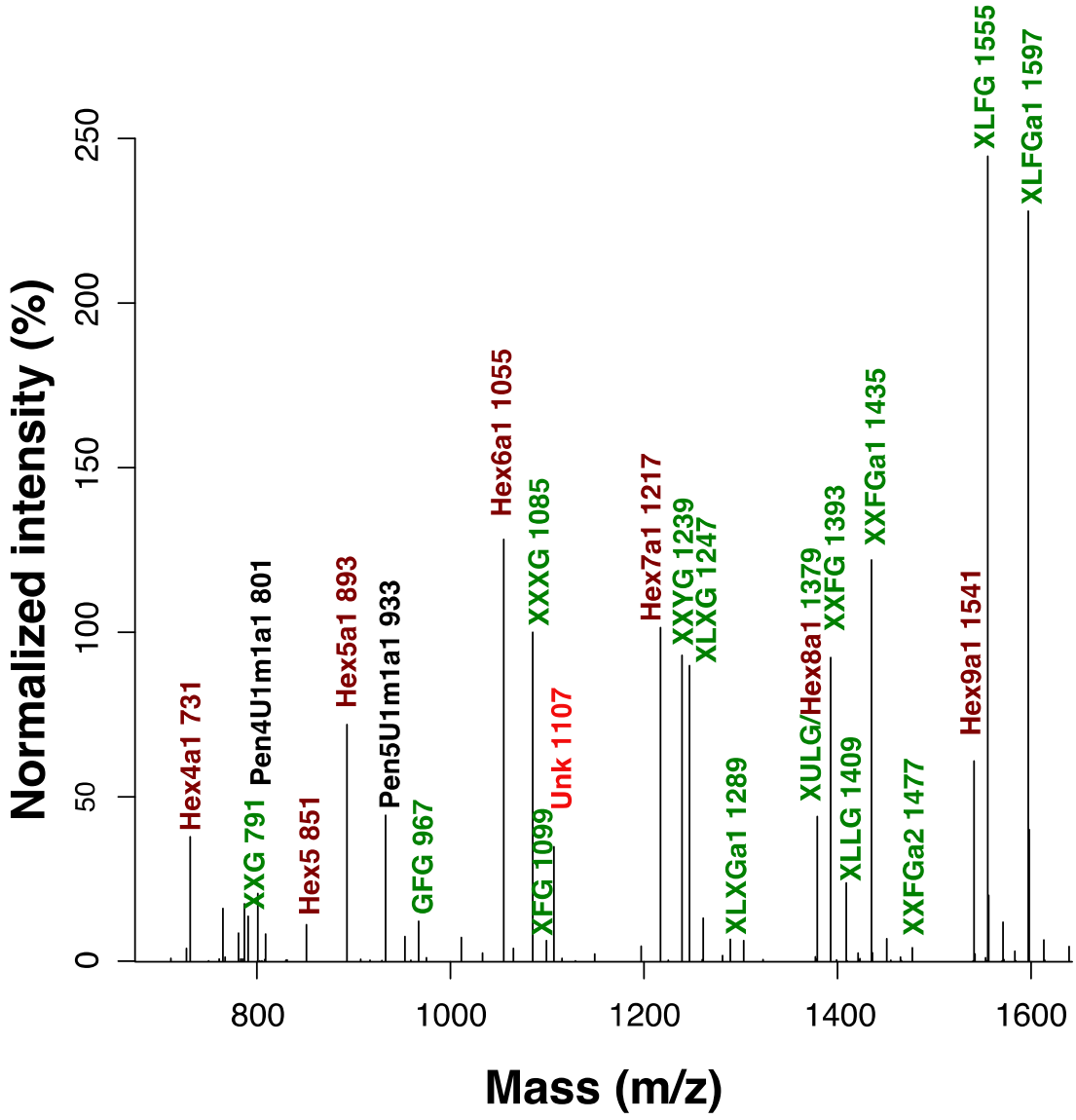

Figure 7 Average MALDI-TOF MS spectrum of sweet cherry glucanase hydrolysate from the entire fruit collection (n= 183). The nomenclature is as described in the text, in Table S1 and Figure S1 followed by the m/z value; in brown: hexose-based oligomers attributed to GgM/β-glucan, in green: XyG oligomer; black: pentose-based oligomers attributed to glucuronoarabinoxylan/glucuronoxylan (GAX/GuX), in red: unknown oligomer. The intensity of ions was normalized to that at m/z 1085 attributed to the XyG structure XXXG.

The PCA of the normalized ion intensities of oligosaccharides relative to that of the ion of the XXXG structure released by glucanase accounted for 43.2% of the variance in the first two components and for 23.3% of the variance in the third and fourth components (Fig. 8A). The first two components distinguished among development stages while the third and fourth components differentiated the two varieties. In the first two components, the contribution of acetylated hexose oligomers was proposed to be related to galactoglucomannan structures: Hex4a1 to Hex9a1 increased up to 420 DD for Garnet and approximately 470 DD for Regina and then decreased (**Fig 8B, Table S5**). GuX oligomers (Pen4u1m1a1) were at their highest levels in the early developing fruit and then decreased to reach a plateau after approximately 300 DD (**Fig 8B, Table S5**). The unidentified oligomer (m/z 1107) had a similar contribution to the profile as Pen4u1m1a1 in Regina (**Fig 8B**). Xyloglucan oligomers contributed more to the oligosaccharide profiles in the later days (**Fig 8A, 8B, Table S5**). Interestingly, a bimodal contribution of XLFG and XLFGa1 structures was detected showing a minimum at approximately 400-600 DD, which is opposite to the maximum of the acetylated hexose oligomers attributed to GgM oligosaccharides (**Fig 8B, Table S5**). The third and fourth components distinguished Garnet from Regina with more important contributions of XyG (XLFG, XXFG) and GgM oligomers of high degree of polymerization (Hex8a1, Hex9a1) in Garnet (**Fig 8A, B**). Besides XLFG, the contribution of XLFGa1 and XXFGa1 differed markedly between in the two cherry cultivars, whereas, as regards ions attributed to GgM (i.e., Hex6a1, Hex9a1), differences were higher between 300-500 DD and opposite for low and high degree of polymerization. GuX oligomers (Pen4u1m1a1), the unknown structure (unk m/z 1107) and diacetylated GgM structures (Hex8a2, Hex9a2) distinguished the two cultivars, particularly during early stages of their development.

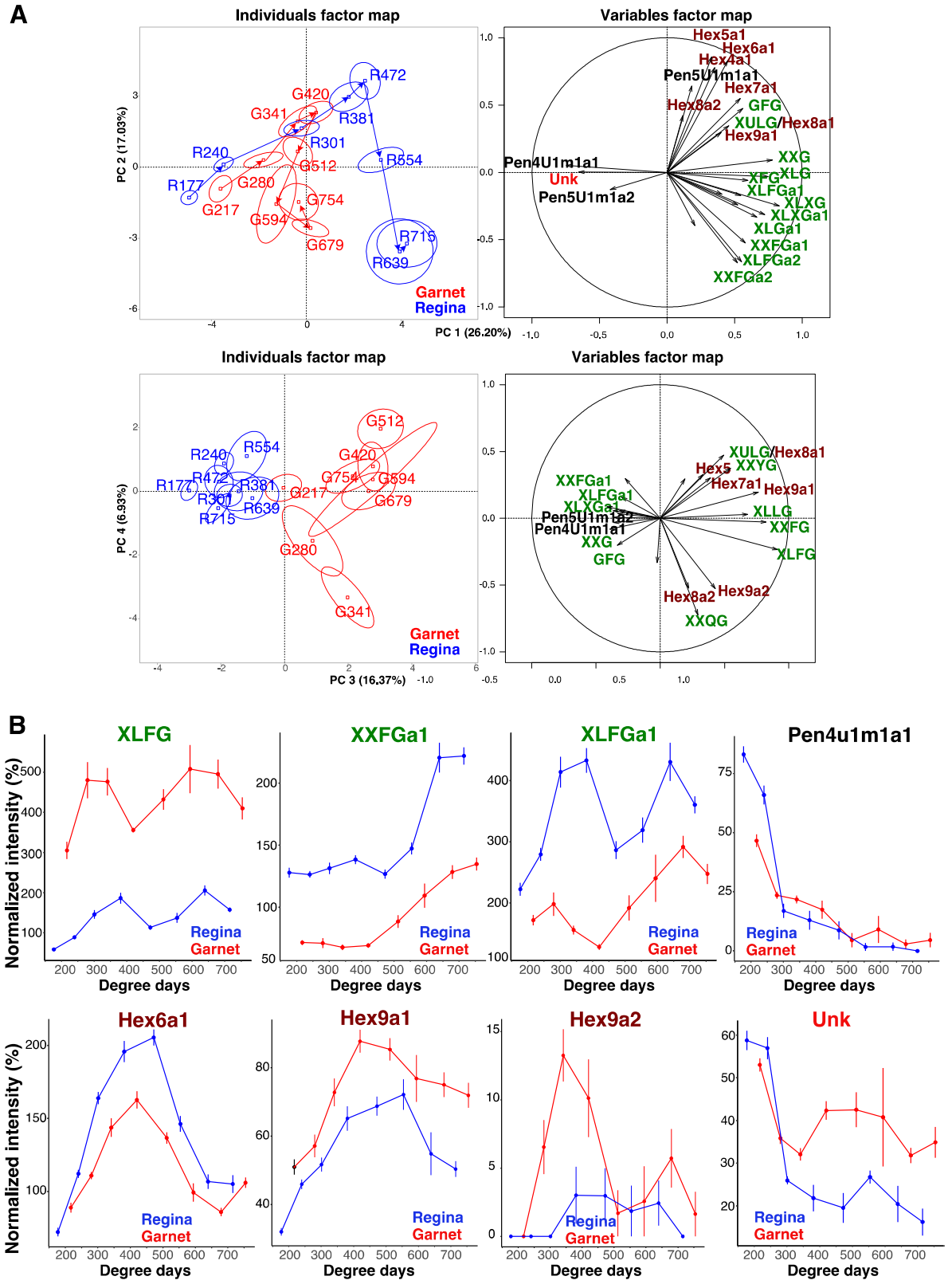

Figure 8 Principal component analysis of MALDI-TOF MS ions attributed to hemicellulose oligomers in the glucanase hydrolysate of AIM from Regina (R) and Garnet (A) according to development (the number following the letter corresponds to the degree-days). A) Principal components 1, 2, 3, 4 (PC1, PC2, PC3, PC4), maps of individuals and variables; B) variation

in relative intensity of characteristic oligosaccharides contributing to PC axes. Nomenclature is as described in the text, Table S1 and Fig S1; Unk: nonidentified oligomer; ellipses in (A) are 95% confidence ellipses for the barycenter of individuals; arrows in (A) and lines in (B) are indicated to guide the eyes to follow changes with fruit development; bars: standard errors; n = 12 except G4 n = 10, G6 n = 6, R7 n = 11.

4 Discussion

4.1 *Pectin structural domains markedly differ in the set setup and evolution of apple and cherry cell walls during fruit development*

The cell wall compositions were within the literature values for apple [19, 22] and cherry [33]. However, they were markedly affected by fruit development: the proportion in the RGI pectin domain increased very early in apple and then decreased to the benefit of the HG domain, while the opposite was observed for cherry after a decrease in cellulose/hemicellulose in very early developmental stages. RGI galactan and arabinan side chains have been related to fruit texture and have long been known to be markedly modified during the late developmental stages (ripening) [6]. Galactan and arabinan are often related to fruit texture (firmness, mealiness) [12, 14, 34], possibly involving both hydrogen binding to cellulose [13] and cell wall water flow since galactan was proposed to limit it [7], while arabinan was found to be more hydrophilic [35]. These side chains are related to apple firmness when the cells are turgid, possibly by limiting slippage of cellulose fibers under tension due to cell turgor pressure, but are detrimental to residual viscoelasticity of the plasmolyzed tissue [14]. Furthermore, the arabinan contribution to apple firmness does not seem to be linked to interactions between linear arabinan and cellulose but more collectively to different types of arabinose linkages in the cell wall [14], including those that may be involved in arabinogalactan proteins reported to participate in fruit softening [36]. Considering that cell expansion starts after approximately 240-270 DD (approximately 45 DAA) [3] in apple, RGI side chains are first very short in very early developmental stages, such as in tomato [20]. RGI then peaked at the beginning of the cell expansion phase to slowly decrease and more noticeably after approximately 1000 DD (after approximately 100 DAA), which is within the apple ripening phase [3]. In contrast, for cherries, after a decrease in hemicellulose/cellulose to a very low proportion (3-5 mol%) after approximately 240-280 DD, the pectin HG structure dominated rapidly (35-40 mol%) after approximately 280-300 DD, while RGI domains increased steadily with fruit development to reach approximately 35

mol% in the ripe fruit. A similar dilution of cellulose content in pectin has already been reported in the cell wall of growing cherry [37]. Fruit softening perception has been related to pectin metabolism/solubilization during ripening [2]. Brittle and soft/melty perception of an apple and a cherry, respectively, can also be related to distinct cell wall organization. In apple, pectin solubilization in ripe fruit is limited and forms a contiguous solid complex remaining when the cellulose-hemicellulose network is removed by enzymatic treatment [38]. Its distribution and hydration within the cellulose-hemicellulose network would control fruit firmness [14]. The richness in HG over RGI domains and a higher ratio of galactose over arabinose as side chains of RGI in the firm Ariane compared to Rome Beauty would agree with a model of cell wall where RGI galactan binding to cellulose contributes to strengthening the cell wall, possibly by limiting cellulose slippage, while hydrated pectin within dispersed cellulose-hemicellulose increases resistance to cell wall compression and by extension, that of the tissue. In contrast, in cherry, the increasing RGI/HG ratio with fruit development with particularly high arabinose content (ratio of Gal/Ara ~ 0.3) would favor of a particularly hydrated cell wall due in part to the presence of hydrophilic arabinan. However, uronic acid richness compared with neutral sugar content in cherry cell walls also appears to be related to firmer texture [39]. Together with a limited cellulose-hemicellulose network, in agreement with [33], the RGI- and arabinan-rich cell wall would be responsible for the soft-to-melting texture of cherry. The increase in pectin rich in RGI domains with arabinan side chains during cherry development would agree with the increase in the ability of the fruit cell wall to take up and retain water (swelling, water holding capacity) during development [37]. However, there was no clear difference supporting the skin cracking susceptibility of the two cultivars. This was most likely due to the global scale at which the present study was realized. The cell wall analyzed (AIM) mainly originated from mesocarp tissue and only slightly originated from epicarp tissue, which is the site of skin cracking. Skin cracking results from microcrack propagation at the cuticle level. It involves the epidermal anticlinal cell wall at the middle lamella and cell wall swelling [40]. The cuticle is a thin complex assembly of cutin, wax, phenolic compounds and polysaccharides [41]. Specific variations in the composition and structure of this barrier leading to different cracking susceptibilities represent a future area of research.

4.2 *Apple and cherry share common glucomannan enrichment at the onset of cell expansion during early fruit development*

Besides global cell wall composition, there was a focus was made on the evolution of hemicellulose structure. In apple, developmental regulation of hemicellulose synthesis and metabolism, notably galactoglucomannan, was observed in early developmental stages [19]. This report confirmed this observation and improved the time-scale resolution, specifying that there was a marked change between approximately 435-760 DD (56-84 DAA) for Rome Beauty and approximately 681 DD (84 DAA) for Ariane, corresponding to the maximum contribution of GgM oligomers to the MALDI-TOF spectra of glucanase hydrolysates. It also corresponded to the maximum mannose and galactose in the cell wall composition. There was a concomitant change in the contribution of the XLFG XyG structure, which peaked very early at approximately 138-174 DD for Ariane and Rome Beauty and then markedly decreased to reach a minimum starting after 345-435 DD for Ariane and Rome Beauty, while its acetylated counterpart, XLFGa1, peaked. It would be of interest to establish whether these nonacetylated and acetylated XyG structures represent markers for dividing versus expanding cells and to identify a role for XyG acetyl esterification in the regulation of apple fruit development, particularly with regard to its interaction with cellulose. Cell expansion is also associated with the XLXGa1 structure, which started increasing in the glucanase hydrolysate during the same period. In fact, this developmental stage appears determinant, as it was close to changes reported in the mechanical properties of apple flesh measured by compression and shear puncture forces [3]. Volz et al. [3] reported a continuous decrease in the compression puncture force in growing Gala apple from young fruits 16 days after full bloom (DAA) to ripe fruit (153 DAA). However, they observed an increase in shear puncture force occurring as two peaks, one after anthesis and a second one at approximately 109-119 DAA depending on the harvest year, followed each time by a decline. If increased cell density may be responsible for the first peak, the authors interpreted the second increase as resulting from a different cell wall setup during this growing phase since there was less wall under the probe as the cell markedly expanded. The peak of GgM oligomers released in the glucanase cell wall hydrolysate and of mannose and galactose in Ariane and Rome Beauty occurring within the same growth period as reported for increased shear puncture force strongly suggest a role of GgM in tissue mechanical properties. Along with this hemicellulose, the peak in the pectin RGI domain and its galactan and arabinan side chains could also contribute to the specific cell wall mechanical properties at the initiation of cell expansion. Of interest is a similar peak in hemicellulose structure attributed to GgM observed in the cell wall glucanase hydrolysate of cherry cell walls at approximately 340-472 DD (40-50 DAA). This period corresponds to stage III in cherry development and is associated with a marked cell expansion [37]. Unlike

apple, XLFG and XLFGa1 XyG oligomers did not peak distinctly with the onset of expansion. Instead, their proportion decreased during this period and resumed during later stages to finally decrease in late fruit development. In contrast with apple, for which the XLXGa1 XyG oligomer proportion increased with cell expansion, it was the proportions of XXFGa1 and its nonacetylated derivative that increased with cell expansion. Marked differences were noted between the hemicellulose oligosaccharide profiles of the two cherry cultivars, as already noted for other Rosaceae [31], confirming the genetic control of XyG structure [22].

The function of GgM in the plant cell wall is diverse. In tomato fruit, it was proposed to be associated with cell-cell adhesion [42], and in a mutant oversynthesizing cell wall mannose, defects were observed in cell division and expansion with softer fruits and fragile stems [43]. GgM interacts with cellulose fibers, which in a model system composed of bacterial cellulose and secondary cell wall GgM led to an increase in the elastic and shear modulus of the composite [17]. This is in line with the reported increase in shear puncture behavior in Gala apple [3] occurring during the same period when the synthesis of GgM was observed to be high [19], and as reported here. GgM helps with cellulose crystallization, aggregation and toughening of bundles, but as observed in composite models, its biomechanical impact also relies on the presence of other cell wall polymers, such as other xylans in the secondary cell wall, and on the fine chemical structure of the hemicelluloses [17]. In the present case, pectin, notably RGI and its side chains together with XyG, which showed remarkable structural changes when GgM oligomers were released most from the cell wall, likely contributed to adapting the cell wall mechanical properties to the cell function. With regard to the contrasting texture in apple, the presence of GgM and its lower metabolism in Rome Beauty, since it contained significantly more mannose and more GgM oligomers were released throughout fruit development compared to Ariane, may lead to cell wall that is resistant to tension and less able to tear apart and to free cellular juice when ripe. Such a situation may contribute to the development of fruit mealiness perception often reported for overripe Rome Beauty. Mealiness involves cell separation instead of cell breakage during flesh destruction [44]. Analogously increased cell wall mechanical resistance may result in the cracking-tolerant cherry cultivar Regina, in which the mesocarp/epicarp cell walls richer in mannose and GgM, than in the susceptible cultivar Garnet. Such mechanical resistance to tension may limit microcrack propagation into macrocracks. Other specific contributions of XyG structures that markedly differed between the two cultivars may also participate in distinguishing the cultivars with regard to their cell wall mechanical properties. Thus, in

addition to other structural differences in the cuticle composition and structure that may be critical for microcrack occurrence and that remain to be established, further work is needed to support the contributions of hemicellulose biosynthesis and metabolism, particularly GgM, to the control of mechanical properties underlying skin cracking in cherry.

5 Conclusion

Analysis of cell wall polysaccharides from brittle apple and soft-textured cherry from the young fruit stage to the ripe fruit allowed the characterization of several features summarized in Figure 9. These merit further studies with regard to contrasting flesh textures and their prediction: the content of cellulose/hemicellulose versus pectin, the ratio of HG and RGI pectin structural domains with the nature of the side chains, and particularly, the fine structure profile of the hemicellulose as revealed by the coupling of cell wall glucanase degradation and MALDI-TOF MS analysis of hydrolysates. This is particularly true for XyG and GgM hemicelluloses, which need to be further assessed as possible markers for cell expansion and whose metabolism may distinguish the texture of the ripe fruit or fruit susceptibility to cracking. In this respect, genes coding for mannan synthase (CLSA), GH9 putative glucanase and galactosidase specific for early fruit development [19] may be worth testing as early markers whose expression levels may help predict apple texture when ripe according to cultivar and growth conditions. Similar approaches could be pursued in cherries following the first gene expression report of developing sweet cherry [45] with regard to the involvement of hemicellulose in skin cracking susceptibility. In addition to the fine structure of GgM, XyG, their acetylation remains to be further assessed concerning their function with regard to cell development and their role in cell wall organization and mechanical properties.

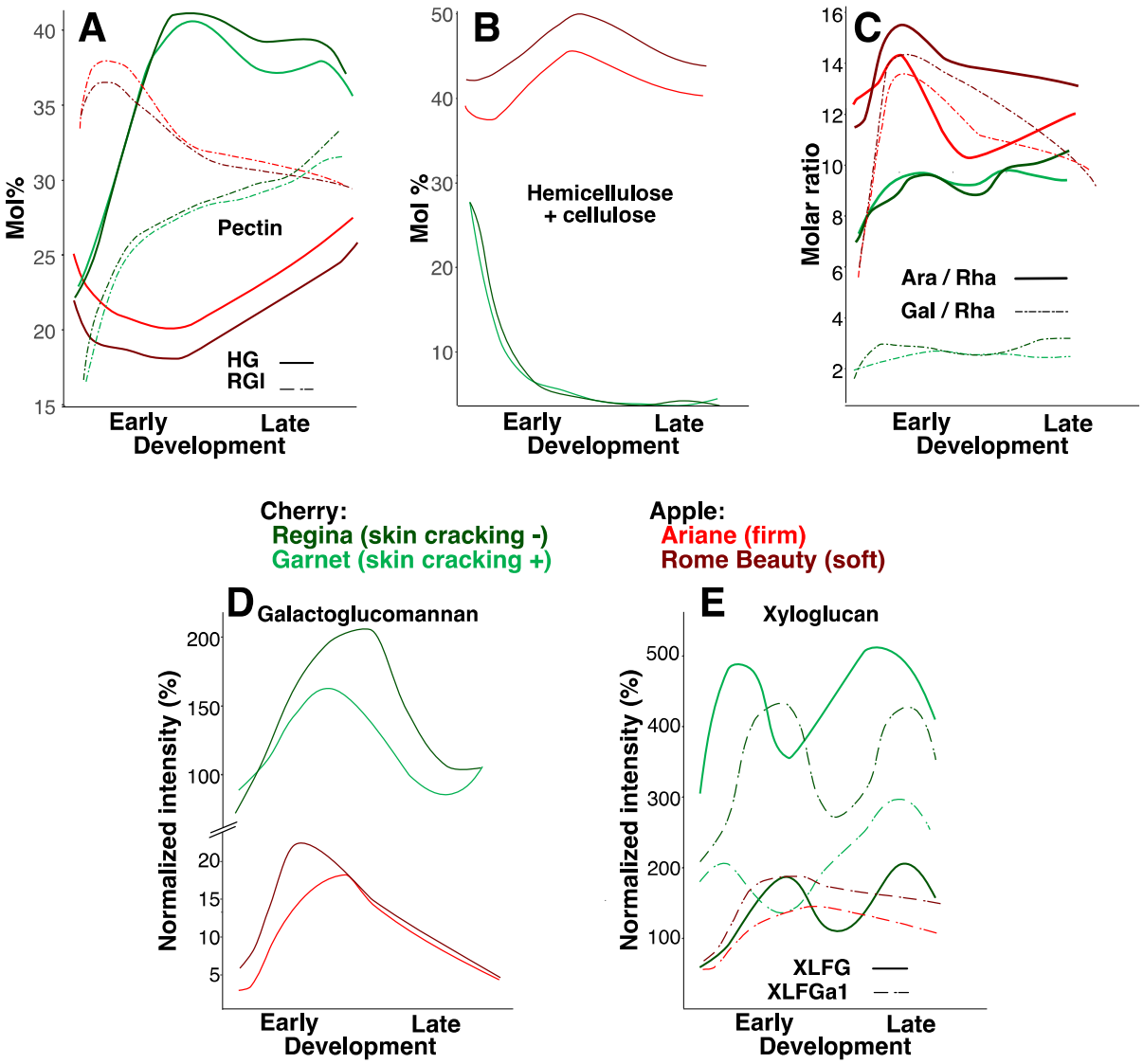

Figure 9 Schematic plots of pectin HG and RGI (A), hemicellulose/cellulose (B) mol proportions, molar ratio of arabinose and galactose to rhamnose representing pectic RGI side chains (C) and evolution of galactoglucomannan (D) and xyloglucan (E) fine structures with fruit development of texture-contrasted apple and sweet cherry with different skin-cracking susceptibilities.

Acknowledgments

Biochemical and MALDI-TOF MS analyses of polysaccharides were performed on the BIBS instrumental platform (https://doi.org/10.15454/1.5572358121569739E12 ; http://www.bibs.inra.fr/ bibs_eng/, UR1268 BIA, IBiSA, Phenome-Emphasis-FR ANR-11-INBS- 0012, PROBE infrastructure, Biogenouest). Sylvain Hanteville, Isadora Rubin de Oliveira, Emna Baïram helped with apple fruits measurements in the field and the laboratory.

The staff of the INRAE experimental unit “Horticulture” at Beaucouzé provided day-to-day maintenance of the orchard. All help is gratefully acknowledged. We thank Bordeaux INRAE Fruit Tree Experimental Unit (UEA), for the management of sweet cherry trees.

Fundings

This work was supported by National Research Institute for Agriculture, Food and Environment and by the Region Pays de la Loire (program AI FRUIT). Activities dealing with sweet cherry were partially funded by the INRAE sweet cherry breeding program, which is supported by INRAE BAP division and by INRAE’s private partner, CEP Innovation.

Bibliography

[1] I. Ben Sadok, A. Tiecher, D. Galvez-Lopez, M. Lahaye, P. Lasserre-Zuber, M. Bruneau, S. Hanteville, R. Robic, R. Cournol, F. Laurens, Apple fruit texture QTLs: year and cold storage effects on sensory and instrumental traits, Tree Genetics & Genomes, 11 (2015) 1-20.

[2] J.A. Mercado, A.J. Matas, S. Posé, Fruit and Vegetable Texture: Role of Their Cell Walls, in: L. Melton, F. Shahidi, P. Varelis (Eds.) Encyclopedia of Food Chemistry, Academic Press, Oxford, 2019, pp. 1-7.

[3] R.K. Volz, F.R. Harker, S. Lang, Firmness decline in 'Gala' apple during fruit development, Journal of the American Society for Horticultural Sciences, 128 (2003) 797-802.

[4] L. Frankova, S.C. Fry, Biochemistry and physiological roles of enzymes that cut and paste plant cell-wall polysaccharides, Journal of Experimental Botany, 64 (2013) 3519-3550.

[5] O.B. Airianah, R.A. Vreeburg, S.C. Fry, Pectic polysaccharides are attacked by hydroxyl radicals in ripening fruit: evidence from a fluorescent fingerprinting method, Ann Bot, 117 (2016) 441-455.

[6] D. Wang, T.H. Yeats, S. Uluisik, J.K.C. Rose, G.B. Seymour, Fruit softening: Revisiting the role of pectin, Trends Plant Sci, 23 (2018) 302-310.

[7] P. Lopez-Sanchez, M. Martinez-Sanz, M.R. Bonilla, F. Sonni, E.P. Gilbert, M.J. Gidley, Nanostructure and poroviscoelasticity in cell wall materials from onion, carrot and apple: Roles of pectin, Food Hydrocolloids, 98 (2020) 105253.

[8] P. Videcoq, A. Barbacci, C. Assor, V. Magnenet, O. Arnould, S. Le Gall, M. Lahaye, Examining the contribution of cell wall polysaccharides to the mechanical properties of apple parenchyma tissue using exogenous enzymes, Journal of Experimental Botany, 68 (2017) 5137-5146.

[9] R.G. Atkinson, P.W. Sutherland, S.L. Johnston, K. Gunaseelan, I.C. Hallett, D. Mitra, D.A. Brummell, R. Schroder, J.W. Johnston, R.J. Schaffer, Down-regulation of POLYGALACTURONASE1 alters firmness, tensile strength and water loss in apple (Malus x domestica) fruit, Bmc Plant Biol, 12 (2012) 129.

[10] M.A. Quesada, R. Blanco-Portales, S. Posé, J.A. García-Gago, S. Jiménez-Bermúdez, A. Muñoz-Serrano, J.L. Caballero, F. Pliego-Alfaro, J.A. Mercado, J. Muñoz-Blanco, Antisense Down-Regulation of the FaPG1 Gene Reveals an Unexpected Central Role for Polygalacturonase in Strawberry Fruit Softening, Plant Physiology, 150 (2009) 1022-1032.

[11] S. Jimenez-Bermudez, J. Redondo-Nevado, J. Munoz-Blanco, J.L. Caballero, J.M. Lopez-Aranda, V. Valpuesta, F. Pliego-Alfaro, M.A. Quesada, J.A. Mercado, Manipulation of strawberry fruit softening by antisense expression of a pectate lyase gene, Plant Physiology, 128 (2002) 751-759.

[12] J.K.T. Ng, R. Schröder, D.A. Brummell, P.W. Sutherland, I.C. Hallett, B.G. Smith, L.D. Melton, J.W. Johnston, Lower cell wall pectin solubilisation and galactose loss during early fruit development in apple (Malus x domestica) cultivar 'Scifresh' are associated with slower softening rate, Journal of Plant Physiology, 176 (2015) 129-137.

[13] D. Lin, P. Lopez-Sanchez, N. Selway, M.J. Gidley, Viscoelastic properties of pectin/cellulose composites studied by QCM-D and oscillatory shear rheology, Food Hydrocolloids, 79 (2018) 13-19.

[14] M. Lahaye, X. Falourd, B. Laillet, S. Le Gall, Cellulose, pectin and water in cell walls determine apple flesh viscoelastic mechanical properties, Carbohydr Polym, 232 (2020) 115768.

[15] T. Zhang, H. Tang, D. Vavylonis, D.J. Cosgrove, Disentangling loosening from softening: insights into primary cell wall structure, Plant J, 100 (2019) 1101-1117.

[16] A. Zykwinska, J.F. Thibault, M.C. Ralet, Competitive binding of pectin and xyloglucan with primary cell wall cellulose, Carbohyd Polym, 74 (2008) 957-961.

[17] J. Berglund, D. Mikkelsen, B.M. Flanagan, S. Dhital, S. Gaunitz, G. Henriksson, M.E. Lindstrom, G.E. Yakubov, M.J. Gidley, F. Vilaplana, Wood hemicelluloses exert distinct biomechanical contributions to cellulose fibrillar networks, Nat Commun, 11 (2020) 4692.

[18] A. Villares, H. Bizot, C. Moreau, A. Rolland-Sabate, B. Cathala, Effect of xyloglucan molar mass on its assembly onto the cellulose surface and its enzymatic susceptibility, Carbohydr Polym, 157 (2017) 1105-1112.

[19] E. Dheilly, S. Le Gall, M.-C. Guillou, J.-P. Renou, E. Bonnin, M. Orsel, M. Lahaye, Cell wall dynamics during apple development and storage involves hemicellulose modifications and related expressed genes, Bmc Plant Biol, 16 (2016) 201.

[20] F. Guillon, A. Moïse, B. Quemener, B. Bouchet, M.-F. Devaux, C. Alvarado, M. Lahaye, Remodeling of pectin and hemicelluloses in tomato pericarp during fruit growth, Plant Science, 257 (2017) 48-62.

[21] N. Obel, V. Erben, T. Schwartz, S. Kuhnel, A. Fodor, M. Pauly, Microanalysis of plant cell wall polysaccharides, Molecular Plant, 2 (2009) 922-932.

[22] D. Galvez-Lopez, F. Laurens, B. Quemener, M. Lahaye, Variability of cell wall polysaccharides composition and hemicellulose enzymatic profile in an apple progeny, International Journal of Biological Macromolecules, 49 (2011) 1104-1109.

[23] G. Winisdorffer, M. Musse, S. Quellec, A. Barbacci, S. Le Gall, F. Mariette, M. Lahaye, Analysis of the dynamic mechanical properties of apple tissue and relationships with the intracellular water status, gas distribution as measured by MRI, histological properties and chemical composition, Postharvest Biology and Technology, 104 (2015) 1-16.

[24] J. Quero-Garcia, P. Letourmy, J.A. Campoy, C. Branchereau, S. Malchev, T. Barreneche, E. Dirlewanger, Multi-year analyses on three populations reveal the first stable QTLs for tolerance to rain-induced fruit cracking in sweet cherry (Prunus avium L.), Hortic Res, 8 (2021) 136.

[25] R.J. Redgwell, E. MacRae, I. Hallett, M. Fischer, J. Perry, R. Harker, In vivo and in vitro swelling of cell walls during fruit ripening, Planta, 203 (1997) 162-173.

[26] J. Anderson, E. Richardson, Utilizing meteorological data for modeling crop and weed growth, Biometeorology in integrated pest management, (1982) 449-461.

[27] S. Le Gall, S. Even, M. Lahaye, Fast estimation of dietary fiber content in apple, J Agric Food Chem, 64 (2016) 1401-1405.

[28] R Core Team, R: A language and environment for statistical computing, in, R Foundation for Statistical Computing, http://www.R-project.org, Vienna, Austria, 2020.

[29] S.T. Tuomivaara, K. Yaoi, M.A. O'Neill, W.S. York, Generation and structural validation of a library of diverse xyloglucan-derived oligosaccharides, including an update on xyloglucan nomenclature, Carbohydrate research, 402 (2015) 56-66.

[30] S. Lê, J. Josse, F. Husson, FactoMineR: An R Package for Multivariate Analysis, Journal of Statistical Software, 25 (2008) 1-18.

[31] M. Lahaye, X. Falourd, B. Quemener, M.F. Devaux, J.M. Audergon, Histological and cell wall polysaccharide chemical variability among apricot varieties, LWT - Food Science and Technology, 58 (2014) 486-496.

[32] M. Lahaye, X. Falourd, B. Quemener, M.C. Ralet, W. Howad, E. Dirlewanger, P. Arus, Cell wall polysaccharide chemistry of peach genotypes with contrasted textures and other fruit traits, J. Agric. Food Chem., 60 (2012) 6594-6605.

[33] G.S. Salato, N.M.A. Ponce, M.D. Raffo, A.R. Vicente, C.A. Stortz, Developmental changes in cell wall polysaccharides from sweet cherry (Prunus avium L.) cultivars with contrasting firmness, Postharvest Biology and Technology, 84 (2013) 66-73.

[34] S.G. Gwanpua, V. Dakwa, P. Verboven, B.M. Nicolai, A.H. Geeraerd, M. Hendrickx, S. Christiaens, B.E. Verlinden, Relationship between texture analysis and texture attributes during postharvest softening of 'jonagold' and 'kanzi' apples, Acta Horticulturae, 1079 (2015) 279-284.

[35] F.H. Larsen, I. Byg, I. Damager, J. Diaz, S.B. Engelsen, P. Ulvskov, Residue specific hydration of primary cell wall potato pectin identified by solid-state 13C single-pulse MAS and CP/MAS NMR spectroscopy, Biomacromolecules, 12 (2011) 1844-1850.

[36] A. Leszczuk, P. Kalaitzis, K.N. Blazakis, A. Zdunek, The role of arabinogalactan proteins (AGPs) in fruit ripening—a review, Horticulture Research, 7 (2020) 176.

[37] C. Schumann, S. Sitzenstock, L. Erz, M. Knoche, Decreased deposition and increased swelling of cell walls contribute to increased cracking susceptibility of developing sweet cherry fruit, Planta, 252 (2020) 96.

[38] R.J. Redgwell, D. Curti, C. Gehin-Delval, Role of pectic polysaccharides in structural integrity of apple cell wall material, European Food Research and Technology, 227 (2008) 1025-1033.

[39] M.F. Basanta, N.M. Ponce, M.L. Salum, M.D. Raffo, A.R. Vicente, R. Erra-Balsells, C.A. Stortz, Compositional changes in cell wall polysaccharides from five sweet cherry (Prunus avium L.) cultivars during on-tree ripening, J Agric Food Chem, 62 (2014) 12418-12427.

[40] C. Schumann, A. Winkler, M. Bruggenwirth, K. Kopcke, M. Knoche, Crack initiation and propagation in sweet cherry skin: A simple chain reaction causes the crack to 'run', PLoS One, 14 (2019) e0219794.

[41] B.P. Khanal, M. Knoche, Mechanical properties of cuticles and their primary determinants, Journal of Experimental Botany, 68 (2017) 5351-5367.

[42] J.J. Ordaz-Ortiz, S.E. Marcus, J.P. Knox, Cell wall microstructure analysis implicates hemicellulose polysaccharides in cell adhesion in tomato fruit pericarp parenchyma, Molecular Plant, 2 (2009) 910-921.

[43] L. Gilbert, M. Alhagdow, A. Nunes-Nesi, B. Quemener, F. Guillon, B. Bouchet, M. Faurobert, B. Gouble, D. Page, V. Garcia, J. Petit, R. Stevens, M. Causse, A.R. Fernie, M. Lahaye, C. Rothan, P. Baldet, GDP-D-mannose 3,5-epimerase (GME) plays a key role at the intersection of ascorbate and non-cellulosic cell-wall biosynthesis in tomato, Plant Journal, 60 (2009) 499-508.

782 [44] S. Mikol Segonne, M. Bruneau, J.M. Celton, S. Le Gall, M. Francin-Allami, M. Juchaux,
783 F. Laurens, M. Orsel, J.P. Renou, Multiscale investigation of mealiness in apple: an atypical
784 role for a pectin methylesterase during fruit maturation, Bmc Plant Biol, 14 (2014) 375.

785 [45] M. Alkio, U. Jonas, M. Declercq, S. Van Nocker, M. Knoche, Transcriptional dynamics
786 of the developing sweet cherry (Prunus avium L.) fruit: sequencing, annotation and
787 expression profiling of exocarp-associated genes, Hortic Res, 1 (2014) 11.

788
789